

# AutoTraces: Autoregressive Trajectory Forecasting via Multimodal Large Language Models

Teng Wang\* Yanting Lu Ruize Wang  
Southeast University

{wangteng, luyanting, wangruize}@seu.edu.cn

## Abstract

We present *AutoTraces*, an autoregressive vision-language-trajectory model for robot trajectory forecasting in human-populated environments, which harnesses the inherent reasoning capabilities of large language models (LLMs) to model complex human behaviors. In contrast to prior works that rely solely on textual representations, our key innovation lies in a novel trajectory tokenization scheme, which represents waypoints with  $\langle \text{point} \rangle$  tokens as categorical and positional markers while encoding waypoint numerical values as corresponding point embeddings, seamlessly integrated into the LLM’s space through a lightweight encoder-decoder architecture. This design preserves the LLM’s native autoregressive generation mechanism while extending it to physical coordinate spaces, facilitates modeling of long-term interactions in trajectory data. We further introduce an automated chain-of-thought (CoT) generation mechanism that leverages a multimodal LLM to infer spatio-temporal relationships from visual observations and trajectory data, eliminating reliance on manual annotation. Through a two-stage training strategy, our *AutoTraces* achieves SOTA forecasting accuracy, particularly in long-horizon prediction, while exhibiting strong cross-scene generalization and supporting flexible-length forecasting.

## 1. Introduction

Forecasting socially compliant trajectories in human-populated environments remains a fundamental challenge for autonomous systems. As mobile robotic platforms are increasingly deployed across campuses, shopping malls, and other public areas, predicting trajectories that adhere to social norms while ensuring safety has become critically important. While deep reinforcement learning (DRL) has dominated prior motion planning research [6, 8, 13, 14, 21, 38, 51], its reliance on trial-and-error learning presents practical limitations for deployment. The recent emergence

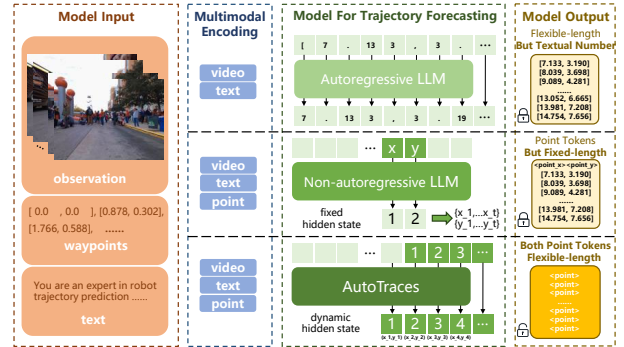


Figure 1. Comparison between our *AutoTraces* and previous LLM solutions. Our method introduces point tokens and embeddings for waypoint representation, enabling autoregressive prediction.

of large-scale human-teleoperated datasets [17, 20, 32, 33, 39] has established “Imitation Learning” as a promising paradigm for socially compliant trajectory forecasting.

Given that visual perception serves as the primary sensory modality for most robotic platforms, the trajectory forecasting task is generally formulated as a multimodal planning problem that integrates historical trajectories with visual observations to generate target-conditioned future waypoints, thereby abstracting away low-level control. Current state-of-the-art (SOTA) imitation learning approaches, including ViNT [42], NoMad [43], and CityWalker [27], typically employ learnable transformer decoders augmented by scene imagination [27, 42] or policy diffusion [43], to predict fixed-length trajectory sequences. Despite considerable advances, these methods demonstrate limited generalization in open-world scenarios. We explain such deficiencies by the limited diversity and scale of expert demonstrations exacerbated by the end-to-end learning paradigm without human-like reasoning in between, hindering genuine understanding of the underlying dynamics.

Inspired by the success of large language models (LLMs) in embodied intelligence [22, 25, 40, 48, 49], we explore a trajectory forecasting framework that harnesses LLMs’ inherent contextual reasoning capability to model complex

\*Corresponding author: Teng Wang.

human behaviors and generate socially compliant trajectories across diverse scenarios. Recent LLM-based methods [2, 23, 30, 44] for general trajectory prediction leverage LLMs’ generative capabilities by framing prediction as QA tasks using *textualized coordinates* (Fig. 1), yet they suffer from token inefficiency and limited spatio-temporal modeling due to excessive coordinate tokenization. Parallel studies in broader spatio-temporal forecasting [24, 31] address this through task-specialized encoders to project structured data into LLM-compatible representations. However, these studies follow the *non-autoregressive* paradigm, generating complete future sequences in a single pass from global representations obtained via static special tokens [24] or flattened hidden states [31], fundamentally limiting the modeling of temporal dynamics and flexible-length forecasting. Furthermore, leveraging visual observations to enhance LLMs’ understanding of complex real-world human behaviors still remains an open challenge.

To tackle these challenges, we present **AutoTraces**, an *autoregressive* vision-language-trajectory model that harnesses multimodal LLMs for socially compliant trajectory forecasting. The key innovation of our AutoTraces lies in a novel trajectory tokenization scheme that effectively bridges the gap between spatio-temporal trajectory patterns with LLMs’ latent representations by introducing unique point embedding paradigm. Our model employs a unified `<point>` token to mark each waypoint—whether historical or future—individually and integrates waypoint values into corresponding point embeddings with textual and visual modalities seamlessly through a lightweight encoder-decoder framework (Fig. 2). This design preserves LLMs’ native autoregressive generation mechanism while extending it to physical coordinate spaces, facilitating long-term interaction modeling in trajectory data. Meanwhile, we introduce Chain-of-Thought (CoT) prompting to further enhance LLMs’ understanding of complex social behaviors in video inputs. Rather than relying on manual annotation, we automate CoT generation by leveraging auxiliary LLM to perform structured reasoning about the underlying spatio-temporal relationships, facilitated by explicit geometric analysis of agent trajectories. Through our proposed two-stage training strategy, AutoTraces demonstrates superior prediction accuracy over existing SOTA methods and enhanced generalization across diverse scenes. Our contributions are summarized as follows.

- We propose a novel trajectory tokenization scheme that uses `<point>` tokens as categorical and positional markers, with waypoint values integrated into the LLM embeddings via an encoder-decoder architecture, enabling autoregressive generation of trajectories with enhanced spatio-temporal modeling.
- We integrate CoT reasoning into dense trajectory prediction through an automated generation mechanism via

multimodal LLMs, enhancing comprehension of complex social behaviors while eliminating manual annotation.

- Experimental results demonstrate our superiority in long-horizon trajectory prediction and cross-scene generalization, while supporting flexible-length forecasting.

## 2. Related Work

**Social Motion Planning.** Early methods primarily relied on handcrafted social rules and geometric constraints [5, 12, 16], but struggled to model nuanced social behaviors in crowded scenarios. While DRL methods [6, 8, 13, 14, 21, 38, 51] advanced the field, their trial-and-error learning paradigm faced deployment challenges. The shift to imitation learning enabled more flexible approaches, such as Panigrahi et al. [35], who fused RGB and LiDAR data through an MLP to predict trajectories. Subsequent transformer-based models—including ViNT [42], NoMad [43], and CityWalker [27]—leveraged historical trajectories and visual context to infer fixed-length future trajectory. However, these methods exhibit limited generalization across diverse social scenarios. Recent LLM-based solutions such as Social-LLaVA [36] focus on generating high-level navigation commands through language-based reasoning. In comparison, our AutoTraces enables autoregressive prediction of waypoints through parameter-efficient adaptation of LLMs using trajectory tokenization scheme.

**LLMs for Spatio-Temporal Forecasting.** A growing research direction explores spatio-temporal forecasting with LLMs, including applications to general trajectory prediction [2, 7, 23, 30, 44] and traffic flow prediction [24, 31]. Among these approaches, one line of work [2, 11, 18, 23, 30, 44] leverages LLMs’ generative capabilities by formulating spatio-temporal forecasting as question-answering tasks with text-based coordinate representations, while another category of methods [24, 31] utilizes LLMs’ encoding capacity to process historical information and generate future predictions through introducing static special tokens [24] or output hidden state flattening [31]. While LLMs have demonstrated strong performance in general time series understanding [15, 19, 26, 28, 50], socially compliant trajectories involve complex spatio-temporal patterns challenging LLMs’ generative ability. We bridge this gap by introducing a structured trajectory tokenization scheme, which preserves LLM’s native autoregressive generation mechanism while extending it to coordinate spaces.

**CoT Prompting for Robotics.** CoT prompting, originally developed to enhance LLM reasoning through step-by-step decomposition [45], has recently been adapted to robotics for improved decision-making and task planning. By breaking down high-level instructions into sequential sub-goals, CoT prompting enables robots to perform multi-step reasoning, improving robustness in dynamic environments [1, 4, 11, 34, 46]. While CoT prompting has proven

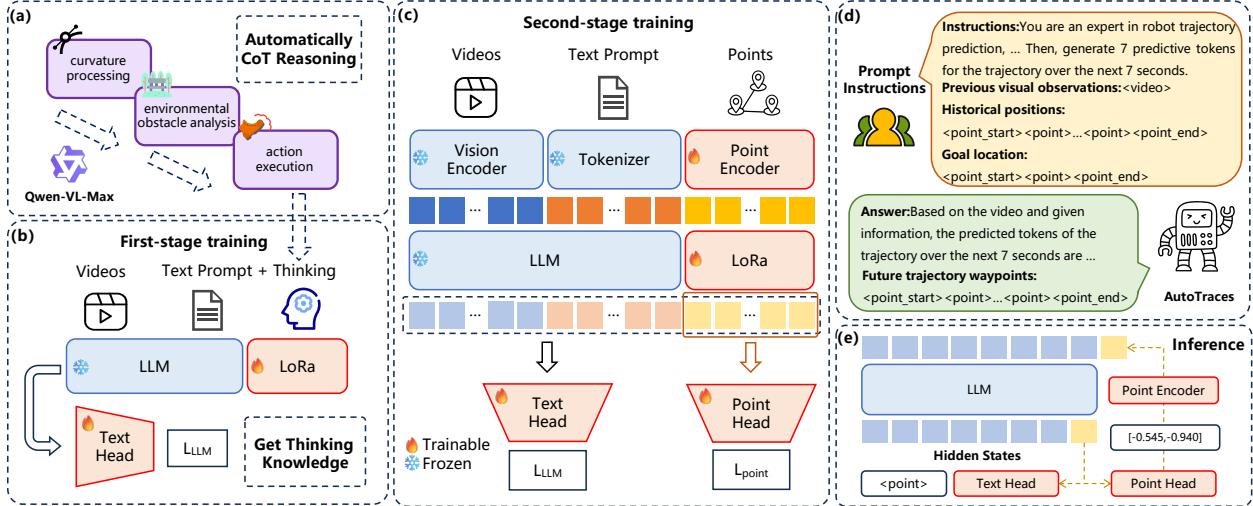


Figure 2. The overall framework of our AutoTraces built upon LLaVa-Video [47] for socially compliant trajectory forecasting. In the first stage, the model is pre-trained on video-text pairs with reasoning prompts to acquire thinking knowledge. The second stage fine-tunes the model using trajectory waypoints (via a Point Encoder), aligning visual observations (via a Vision Encoder) and goal locations (via a Point Encoder). During inference, the model generates future trajectory waypoints as  $\langle \text{point} \rangle$  tokens, enabling autoregressive predictions.

effective for high-level task decomposition and skill sequencing in robotics, its potential for dense trajectory prediction remains largely unexplored. To this end, we introduce automated CoT reasoning to trajectory generation by integrating geometric reasoning.

### 3. Method

#### 3.1. Overall Framework

We focus on socially compliant trajectory forecasting in human-populated environments by learning from a corpus of expert demonstrations. We formulate the task as a sequence generation task conditioned on multimodal inputs. At each time step  $t$ , the agent receives a RGB observation  $\mathbf{o}_t \in \mathbb{R}^{H \times W \times 3}$ , its current position  $\mathbf{x}_t \in \mathbb{R}^2$ , and the goal location  $\mathbf{g} \in \mathbb{R}^2$ . The agent aims to generate a sequence of future trajectory waypoints  $\mathbf{x}_{t+1:t+T} = \{\mathbf{x}_{t+1}, \dots, \mathbf{x}_{t+2}, \mathbf{x}_{t+T}\}$  in Euclidean space conditioned on the previous visual observations  $\mathbf{o}_{t-L:t} = \{\mathbf{o}_{t-L}, \dots, \mathbf{o}_{t-1}, \mathbf{o}_t\}$ , positional information  $\mathbf{x}_{t-L:t} = \{\mathbf{x}_{t-L}, \dots, \mathbf{x}_{t-1}, \mathbf{x}_t\}$  and the goal position  $\mathbf{g}$ . Typically, we take  $L = 8$  and  $T$  varies to adapt to different navigation scenarios and robot configurations.

As shown in Fig. 2, we present AutoTraces, an autoregressive vision-language-trajectory model built upon LLaVa-Video [47]. The model accepts a structured prompt that unifies historical waypoints and target goals into a shared  $\langle \text{point} \rangle$  token space to ensure trajectory consistency, while incorporating video metadata (e.g., sequence length, frame rate) to enhance contextual reasoning. This formulation enables the model to interpret navigation con-

texts and generate trajectories of variable length as required. Furthermore, CoT reasoning is incorporated as a pre-training task to enhance AutoTraces’s understanding of complex social interactions. The model is efficiently fine-tuned using Low-Rank Adaptation (LoRA) for both trajectory prediction and CoT reasoning tasks.

#### 3.2. Trajectory Tokenization

We propose an autoregressive multimodal LLM framework for flexible-length trajectory prediction. Departing from methods that directly output numerical coordinates as text [2, 23, 30, 44], we introduce a structured tokenization scheme: a special  $\langle \text{point} \rangle$  token is used to represent each 2D waypoint  $\mathbf{x}_t \in \mathbb{R}^2$ , while  $\langle \text{point\_start} \rangle$  and  $\langle \text{point\_end} \rangle$  tokens demarcate trajectory boundaries. These tokens are integrated into the LLM model LLaVa-Video by extending the original vocabulary, effectively treating trajectory waypoints as a new output modality within the generative language framework.

To seamlessly integrate trajectory waypoints with textual and visual modalities, we design a lightweight encoder-decoder framework that operates directly in the LLM’s native representation space. Specifically, we first introduce a *Point Encoder* that represents waypoints using Transformer-style positional encoding, then feed them into MLPs, mapping physical coordinates into the LLM’s latent space at each time step  $t$ ,

$$\mathbf{e}_{t-i} = \text{PointEncoder}(\mathbf{x}_{t-i}), \quad i = L, \dots, 0 \quad (1)$$

where  $\mathbf{x}_{t-i} = (x_{t-i}, y_{t-i}) \in \mathbb{R}^2$  and  $\mathbf{e}_{t-i} \in \mathbb{R}^D$  represents the  $i$ -th historical waypoint and its encoded embedding, re-

spectively. This mapping enables unified processing of trajectory, visual, and textual tokens in a shared feature space. The LLM takes as input a multimodal sequence comprising: (1) historical waypoint embeddings  $\mathbf{E}_t = \{\mathbf{e}_{t-i}\}_{i=L}^0$ , (2) visual embeddings  $\mathbf{V}_t = \{\mathbf{v}_{t-i}\}_{i=L}^0$ , where  $\mathbf{v}_{t-i}$  encodes the visual observation  $\mathbf{o}_{t-i}$ , and (3) text prompt embeddings  $\mathbf{P}_t$ . Through autoregressive decoding, the model generates a sequence of  $F$  future waypoint embeddings:

$$\{\hat{\mathbf{e}}_{t+1}, \dots, \hat{\mathbf{e}}_{t+T}\} = \text{LLM}(\mathbf{E}_t, \mathbf{V}_t, \mathbf{P}_t), \quad (2)$$

where  $\hat{\mathbf{e}}_{t+k} \in \mathbb{R}^D, k \in \{1, 2, \dots, F\}$ , refers to the output feature embeddings of the  $k$ -th future waypoint. Finally, we decode the predicted waypoint embeddings back to physical coordinates via a *Point Head*:

$$\hat{\mathbf{x}}_{t+k} = \text{PointHead}(\hat{\mathbf{e}}_{t+k}), \quad k = 1, \dots, T \quad (3)$$

with  $\hat{\mathbf{x}}_{t+k} = (\hat{x}_{t+k}, \hat{y}_{t+k}) \in \mathbb{R}^2$  denoting the coordinate of the predicted  $k$ -th future waypoint. Such an encoder-decoder design enables the `<point>` modality to be naturally integrated into the LLM’s token space without requiring architectural modifications to the base transformer. Our framework extends the LLM’s autoregressive mechanism to physical coordinate, supporting structured waypoint prediction within a unified generative paradigm. Architectural details of point encoder/decoder are given in the **Appendix**.

### 3.3. Chain-of-Thought Reasoning with VLMs

To enhance the visual reasoning capability for complex behavioral understanding in video sequences, we introduce automatically generated Chain-of-Thought (CoT) reasoning as an intermediate representation. Rather than relying on manual annotation, we employ Qwen-VL-Max [3], a powerful visual-language model, to produce CoT content directly from visual observations and trajectory data. Our approach not only eliminates the need for costly human labeling but also provides interpretable behavioral analysis that bridges visual perception and trajectory prediction.

Specifically, our CoT generation framework employs a structured prompting strategy that grounds reasoning in multimodal trajectory dynamics. We provide Qwen-VL-Max with synchronized inputs comprising ground-truth future trajectories and partial historical trajectories, along with their corresponding visual observations. In particular, we also incorporate explicit trajectory curvature analysis to facilitate Qwen-VL-Max for social reasoning, as illustrated in Fig. 3. The curvature processing utilizes a sliding-window mechanism to decompose future trajectories into locally coherent segments, each categorized by directional patterns (e.g., “straight,” “left,” “right”). This decomposition transforms continuous motion into a discrete meta-action sequence, whose symbolic representation structurally guides the reasoning generation while maintaining consistency between physical motion and linguistic rationale. The reasoning process follows a two-stage

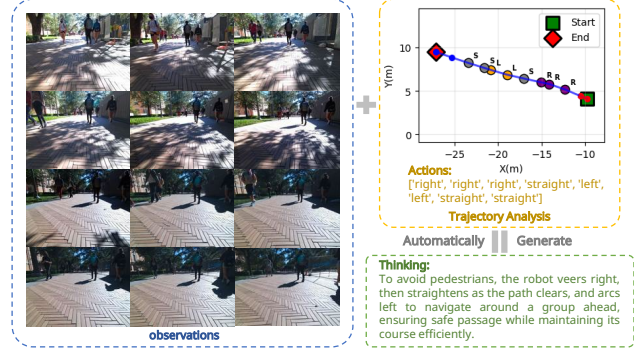


Figure 3. Illustration of the CoT generation for AutoTraces, incorporating visual observations and trajectory analysis. Red points and lines denote the historical trajectory, while blue points and lines denote the ground-truth trajectory. Action annotations (R: right, L: left, S: straight) are marked along the trajectory.

paradigm—environmental obstacle analysis followed by executable action derivation—ensuring each navigational decision remains visually grounded and logically traceable.

### 3.4. Training and Inference

**Autoregressive Prediction.** Our AutoTraces fully leverage the autoregressive generation capability of LLMs to predict trajectories of theoretically arbitrary length. Rather than operating solely on `<point>` tokens, we retain the native textual and visual modalities (Fig. 2 (d)), thereby preserving the model’s pre-trained reasoning and task comprehension abilities to support trajectory prediction. Given a multimodal sequence of video, text, and historical `<point>` tokens, the objective for the model is to generate a subsequent sequence of future `<point>` tokens, the quantity of which must precisely match the requirement specified in the prompt instruction. As illustrated in Fig. 2 (e), upon generating a `<point>` token, it is routed to the *Point Head* module, which decodes the corresponding hidden states into a waypoint coordinate. This coordinate is then processed by the *point encoder* and appended to the input sequence. The updated sequence is fed back into the LLM to continue autoregressive generation until the model outputs the `</s>` (end-of-sequence) token, indicating the trajectory is complete. This autoregressive generation mechanism, where each newly predicted waypoint is immediately fed back to inform the next prediction, significantly enhances the model’s capacity for long-horizon reasoning.

**Two-stage Training.** Our training pipeline employs a two-stage strategy designed to progressively instill visual reasoning capabilities while preserving the LLM’s inherent knowledge. As illustrated in Fig. 2, the first stage focuses on learning interpretable reasoning patterns by taking historical observations  $\mathbf{o}_{t-L:t}$  and past coordinates  $\mathbf{x}_{t-L:t}$  as inputs to generate structured CoT rationales. This de-

Table 1. Performance evaluation of trajectory prediction over 5 to 10 steps on SCAND dataset [20], with an interval of 1s per step. Baselines with gray background are specifically trained and tested on fixed trajectory lengths. In contrast, “Single Model” variants are predominantly trained on T=10 sequences (except NoMad trained on T=8) and evaluated across all horizons under truncated-length settings.

Method	Single Model	T=5		T=8		T=10	
		L2 (m)↓	L1 (m)↓	L2 (m)↓	L1 (m)↓	L2 (m)↓	L1 (m)↓
GNM [41]	✗	0.855	1.034	1.908	2.362	1.708	2.164
GNM [41]	✓	0.895	1.122	1.456	1.826	1.708	2.164
ViNT [42]	✗	0.973	1.168	1.430	1.754	1.714	2.132
ViNT [42]	✓	0.908	1.106	1.435	1.762	1.714	2.132
NoMad [43]	✗	1.167	1.440	1.625	2.102	–	–
NoMad [43]	✓	1.060	1.318	1.625	2.102	–	–
CityWalker [27]	✗	0.995	1.264	1.276	1.610	1.407	1.806
CityWalker [27]	✓	0.862	1.096	<u>1.240</u>	<u>1.572</u>	<u>1.407</u>	<u>1.806</u>
LLaVa-Video [47]	✓	1.007	1.242	1.548	1.918	1.963	2.412
<b>AutoTraces (ours)</b>	✓	<b>0.674</b>	<b>0.856</b>	<b>0.923</b>	<b>1.190</b>	<b>1.089</b>	<b>1.384</b>

sign explicitly decouples reasoning acquisition from trajectory prediction, allowing the model to leverage the LLM’s pretrained knowledge while learning to ground visual and spatial contexts into coherent reasoning traces. At this stage, following standard LLM practice, we optimize the *LoRA* layers and *Text Head* using the standard cross-entropy loss, since model outputs are confined to text tokens. This CoT pre-training provides superior initialization for the LoRA weights over random initialization, thereby enhancing learning in the subsequent trajectory forecasting stage. In the second stage, we specialize the inherited model for trajectory forecasting by integrating the `<point>` modality into the native textual and visual modalities. To address the limitation of cross-entropy loss for regression—where it treats digits as discrete classifications and ignores error magnitude—we augment the objective with a trajectory point loss  $\mathcal{L}_{\text{point}}$  to provide direct regression supervision on the output waypoints. The second-stage objective combines trajectory regression and sequence generation losses:

$$\mathcal{L}_{\text{point}} = \frac{1}{F} \sum_{i=t+1}^{t+F} \|\mathbf{x}_i - \hat{\mathbf{x}}_i\|_1, \quad (4)$$

$$\mathcal{L}_{\text{total}} = \mathcal{L}_{\text{point}} + \mathcal{L}_{\text{LLM}},$$

where  $\mathcal{L}_{\text{LLM}}$  (cross-entropy) ensures the output sequence structure and length, while  $\mathcal{L}_{\text{point}}$  ensures waypoint prediction accuracy. Parameter updates are confined to the *LoRA* layers, *Text Head*, *Point Encoder* and *Point Head*.

## 4. Experiments

### 4.1. Experiment Settings

**Datasets and Evaluation Metrics.** We evaluate our AutoTraces on the benchmark SCAND dataset [20], a social navigation dataset capturing complex human-robot interac-

tions in crowded public spaces. To assess cross-scene generalization, we further conduct experiments on two distinct real-world datasets: GoStanford [17] for indoor and RECON [39] for outdoor scenarios. Following prior work [27], we employ both L2 and L1 distances for evaluation. The L2-distance measures the average Euclidean displacement error between predicted and ground-truth trajectories, while the L1-distance provides robustness to outliers by computing the mean absolute error.

**Implementation Details.** All experiments are conducted on NVIDIA RTX 4090 GPUs. We construct our dataset from SCAND [20], containing 24,512 training and 2,672 testing samples with strictly disjoint trajectories. We adopt the  $160 \times 120$  image resolution from ViNT [42], and sample the data at 1 Hz. Each training sample uses a history of 8 steps and a future horizon randomly averaged between 5-10 steps, with a 1s interval per step. Our method is based on LLaVA-NeXT-Video-7B [47], with its visual encoder CLIP [37] and projector kept frozen. We employ a two-stage QLoRA [10] fine-tuning strategy. Stage 1: 2 epochs, batch size 4, learning rate  $2 \times 10^{-5}$ . Stage 2: 10 epochs, batch size 4, learning rate  $2 \times 10^{-4}$ . Both stages use AdamW-8bit [9, 29], a cosine scheduler with 0.01 warmup, and LoRA rank  $r = \alpha = 32$ .

**Baselines.** We consider several SOTA baseline methods for performance comparison, including GNM [41], ViNT [42], NoMad [43], CityWalker [27], and LLaVa-Video [47]. The first four methods are specifically designed for robot trajectory prediction, while LLaVa-Video [47] exemplifies text-only adaptation of large vision-language models to trajectory forecasting, where continuous coordinates are serialized into discrete textual tokens for generative modeling. For non-autoregressive models (GNM, ViNT, NoMad, CityWalker), we consider two variants for fair comparison: (1) models specifically trained for individual hori-

Table 2. Performance evaluation of cross-scene trajectory prediction on unseen GoStanford dataset [17] for indoor and RECON dataset [39] for outdoor scenarios with prediction horizon ranging from 5 to 10 steps, with an interval of 1s per step.

Methods	Benchmark	T=5		T=8		T=10	
		L2 (m)↓	L1 (m)↓	L2 (m)↓	L1 (m)↓	L2 (m)↓	L1 (m)↓
GNM [41]	GoStanford	3.375	4.164	5.018	6.186	6.022	7.413
	RECON	1.754	2.328	3.141	4.168	4.117	5.448
ViNT [42]	GoStanford	2.980	3.688	4.320	5.348	5.192	6.378
	RECON	1.804	2.406	3.158	4.206	4.151	5.510
NoMad [43]	GoStanford	3.470	4.252	5.108	6.224	–	–
	RECON	1.755	2.316	3.096	4.098	–	–
CityWalker [27]	GoStanford	1.407	1.784	2.112	2.682	2.641	3.348
	RECON	1.955	2.500	3.082	3.938	3.877	4.966
LLaVa-Video [47]	GoStanford	1.090	1.378	1.697	2.144	2.141	2.710
	RECON	1.943	2.472	3.289	4.182	4.211	5.358
AutoTraces (Ours)	GoStanford	1.035	1.312	1.502	1.912	1.772	2.240
	RECON	1.547	1.974	2.302	2.936	2.837	3.614

zon lengths, and (2) unified models trained exclusively with T=10 (except NoMad trained on T=8) and evaluated across all horizons under truncated-length settings. Unless otherwise specified, the unified models are used by default in the experiments. Please note that we exclude existing non-autoregressive LLM methods [24, 31] due to their incompatible task-specific encoders, but include a non-autoregressive variant in ablation studies to validate the advantage of autoregressive generation.

## 4.2. Main Results

We present a comprehensive evaluation of trajectory prediction performance across varying horizons (T=5, 8, 10) in Tab. 1. It could be noticed that our AutoTraces achieves SOTA performances across all evaluation metrics. For short-term prediction ( $T = 5$ ), AutoTraces attains L2 and L1 errors of 0.674m and 0.856m, respectively, surpassing the best-performing baseline GNM by 0.181m (L2) and 0.178m (L1). This advantage further amplifies in long-horizon settings. Specifically, AutoTraces achieves L2 and L1 errors of 1.089m and 1.384m at T=10 respectively, outperforming the second-performing CityWalker by 0.318m (L2) and 0.422m (L1). These results demonstrate the efficacy of our autoregressive approach in preserving prediction accuracy over extended time horizons. Additionally, our AutoTraces demonstrates significant superiority over LLaVA-Video across all prediction horizons, validating the effectiveness of our proposed trajectory tokenization scheme combined with the CoT reasoning.

## 4.3. Cross-Scene Trajectory Prediction

As shown in Tab. 2, we evaluate the generalization capability of all methods on two unseen datasets: GoStanford (indoor) and RECON (outdoor). The results demonstrate

a clear advantage of autoregressive approaches—our AutoTraces and LLaVa-Video—over non-autoregressive baselines such as GNM, ViNT, NoMad, and CityWalker. This suggests that modeling trajectory prediction as an autoregressive decision-making process better captures temporal dependencies and leads to more robust performance in unseen scenes. Among autoregressive methods leveraging large foundation models, our AutoTraces consistently outperforms LLaVa-Video across all prediction horizons and benchmarks, with particularly notable gains observed in long-term prediction (T=10). Specifically, on the indoor GoStanford dataset, we achieve an L2 of 1.502 at T=8 and 1.772 at T=10, compared to LLaVa-Video’s 1.697 and 2.141, respectively. Similar trends are observed in outdoor RECON scenes, where our method reduces L2 error by 30.0% at T=8 and 32.6% at T=10. This significant superiority of AutoTraces over LLaVa-Video validate the effectiveness of our trajectory tokenization scheme and CoT reasoning in enabling more generalizable trajectory forecasting.

## 4.4. Extending to Long-term Trajectory Prediction

We further evaluate our model’s generalization to long-term prediction horizons, as this flexible-length forecasting capability directly reflects its adaptability to diverse robotic platforms with varying velocities. We consider LLaVa-Video [47] for performance comparison. We report the **Instruction Execution Accuracy (IEAcc)** and **Tokens Per Response (TPR)**, combined with the average L2 and L1 errors under accurate execution (**L2@S** and **L1@S**) for each method. Specifically, IEAcc quantifies the model’s capability to generate trajectories of the required length, while TPR measures the token count for a trajectory inference, which is hardware-independent and provides a consistent indicator of model efficiency. Our AutoTraces model

Table 3. Performance Comparison of Extended Trajectory Prediction on SCAND [20] with prediction horizon over 12-20 steps (1s/step).

Horizon	LLaVa-Video [47]				AutoTraces (Ours)			
	L2@S (m)↓	L1@S (m)↓	IEAcc	TPR	L2@S (m)↓	L1@S (m)↓	IEAcc	TPR
12	1.653	2.086			1.611	2.046		
15	2.057	2.597			1.857	2.354		
18	2.426	3.055	40.34%	375.64	2.124	2.692	99.92%	25.00
20	2.584	3.244			2.324	2.950		

was fine-tuned for only one epoch on a dataset comprising 1,336 samples (one-eighth of the total dataset), whereas LLaVA-Video was fine-tuned for one epoch on twice the amount of our data, each with a sequence length of 20. As shown in Table 3, our model achieves significantly higher instruction-following accuracy, attaining 99.92% compared to 40.34%, while achieving lower L1/L2 errors across all horizons under truncated-length settings. The instruction-following failures from LLaVa-Video primarily manifest as: (1) violation of length specifications, (2) failure to terminate generation, and (3) introduction of abnormal spatial dimensions (*e.g.*, introducing a z-coordinate in (x,y) trajectories). The above superiority of our AutoTraces could be attributed to our point modality encoding mechanism, which facilitates the model’s understanding of trajectory coordinates, enabling effective generalization across different scenarios with minimal fine-tuning samples and fine-tuning time, thereby significantly reducing computational costs. Consequently, for new domain adaptation, the entire language model requires no extensive retraining. Only the specialized prediction module and LoRA need lightweight fine-tuning, thereby leveraging the base model’s pre-trained knowledge synergistically. Another key advantage of our point encoding mechanism is a dramatic reduction in TPR (25 vs. LLaVA-Video’s 375). By representing each waypoint with a single token—unlike widely adopted text-based methods that require multiple tokens per coordinate—we provide an efficient pathway for numerical prediction in LLMs.

#### 4.5. Ablation Study

**Effectiveness of Main Components.** We conduct a comprehensive ablation study to evaluate the contributions of two key components in our AutoTraces: the waypoint embedding paradigm and the Chain-of-Thought (CoT) reasoning module. As shown in Fig. 4, we compare three configurations on the SCAND [20] dataset: our full method (Ours), our method without CoT reasoning (Ours w/o CoT), and a baseline method LLaVa-Video that employs pure text representation for waypoints. The results demonstrate that our full method achieves superior performance across varying sample lengths, consistently maintaining the lowest L2 distance. Even without CoT reasoning, our method shows significant improvement over LLaVa-Video. For in-

stance, at T=10, our method achieves an L2 distance of 1.145, substantially lower than LLaVa-Video’s 1.963. This demonstrates the fundamental advantage of our learnable token representation over pure text encoding for waypoint modeling. In addition, the performance gap between our full model and the ablated version (Ours w/o CoT) clearly demonstrates the contribution of the CoT reasoning module.

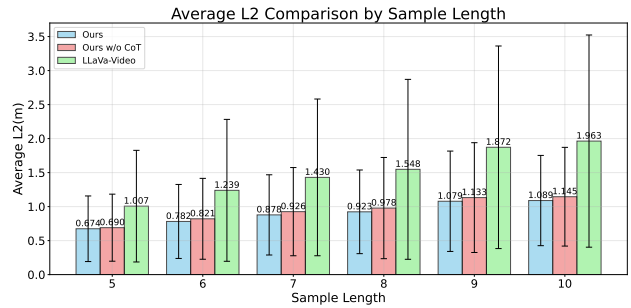


Figure 4. Ablation study of our learnable waypoint tokenization scheme and CoT reasoning on SCAND [20] dataset.

**Autoregressive vs. Single-pass Predictions.** We conduct an ablation study on our model using a similar strategy as UrbanGPT [24] (see Fig. 1, middle) to illustrate the effectiveness of autoregressive prediction. To be precise, we employ two fixed points to represent the x- and y-coordinates, and leverages fixed hidden states to decode trajectories of predetermined sequence lengths. As shown in Fig. 6, on the SCAND dataset, our method achieves slightly better performance compared to the fixed model. Benefiting from the advantages of our point encoding strategy, the fixed model also achieves impressive performance. In contrast, on the completely unseen RECON dataset, our autoregressive method demonstrates significantly stronger generalization, consistently outperforming the fixed-length baseline across all prediction horizons. This structural advantage stems from our point-wise autoregressive design, which ensures seamless alignment between historical and future waypoints during encoding and decoding, whereas the fixed method suffers from an encoder-decoder misalignment due to their decoupled design. This autoregressive forecasting mechanism with its inherent trajectory consis-

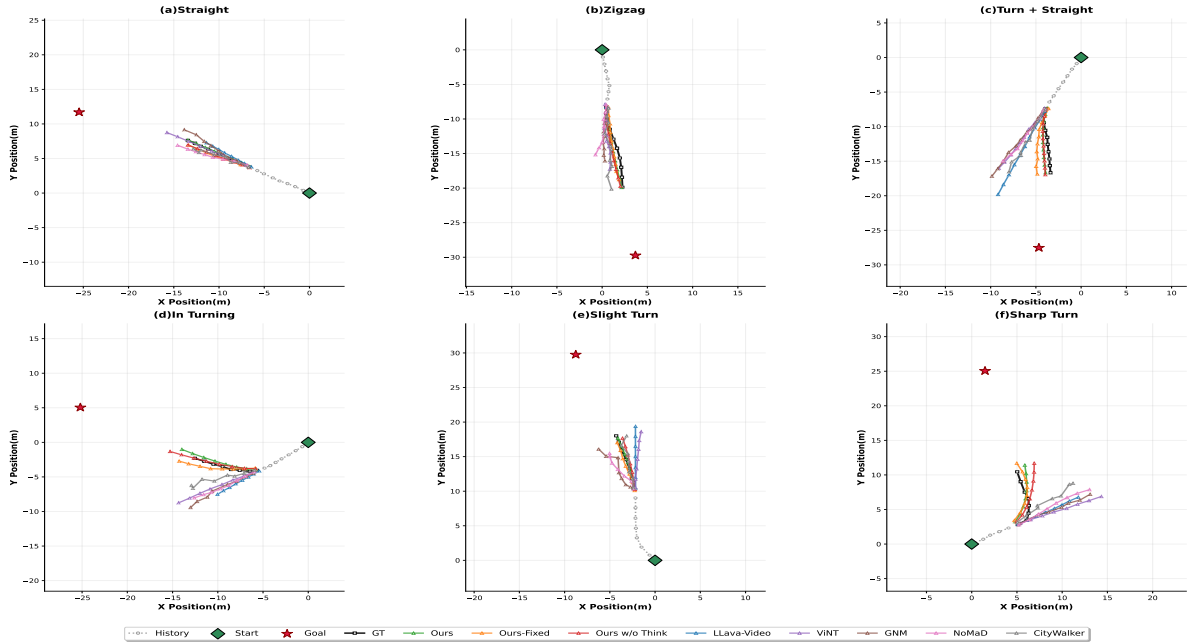


Figure 5. Visualizations of predicted trajectory from our AutoTraces and other baselines on SCAND [20] dataset.

tency enables better adaptation to dynamics variations (e.g., velocity), leading to stronger cross-domain generalization.

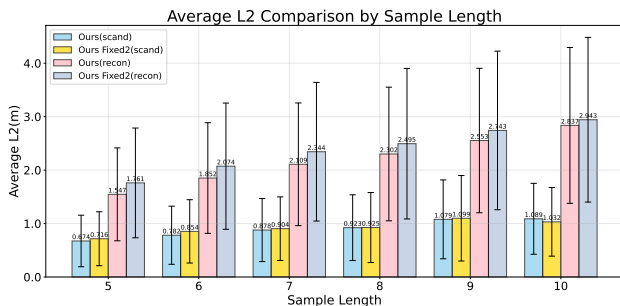


Figure 6. Comparison between autoregressive and one-pass predictions on SCAND [20] and RECON [39] datasets.

#### 4.6. Visualizations of Predicted Trajectory

For an intuitive comparison, we visualize the predicted trajectories of different models in Fig. 5, which presents six representative navigation scenarios. In Fig. 5 (a), depicting smooth forward movement, all models correctly predict the direction, with our model achieving the highest accuracy. Fig. 5 (b) illustrates a zigzag path typical of crowded environments, where none of the models adequately adjust their directions, resulting in unsatisfactory predictions. In the remaining subfigures Fig. 5 (c)–(f), we focus on the models’ performance in predicting turns of varying degrees. It can be observed that most non-LLM-based models fail to anticipate turning tendencies in most cases. In Fig. 5 (e), a few

non-LLM-based models perceive the turning intention in the slight turn scenario, only CityWalker accomplishes the turning maneuver, even though its trajectory accuracy remains suboptimal. In contrast, our LLM-based model effectively recognizes potential turning situations, leading to significantly improved trajectory prediction. Notably, LLaVA-Video, which relies solely on textual input, fails to produce reasonable turning behavior. This finding highlights the importance of the point modality in our model, which effectively guides trajectory prediction by integrating trajectory information with visual and textual information. Furthermore, the full model consistently achieves higher precision compared to its ablated versions across all scenarios.

## 5. Conclusion

We introduced AutoTraces, an autoregressive vision-language-trajectory model built upon multimodal LLMs. Our approach integrates spatio-temporal trajectory data with LLM reasoning through a novel tokenization scheme that maps waypoints to special tokens and corresponding embeddings, preserving autoregressive generation while extending it to physical trajectory spaces. A lightweight encoder-decoder aligns trajectories with visual and textual inputs, and an automated CoT mechanism infers spatio-temporal relationships without manual annotation. Experiments show that AutoTraces achieves SOTA accuracy and remarkable cross-scene generalization, while supporting flexible-length predictions.

## Acknowledgment

This work was supported by the National Natural Science Foundation of China (Grant No.62273093).

## References

- [1] M. Ahn, A. Brohan, N. Brown, Y. Chebotar, O. Cortes, B. David, C. Finn, C. Fu, K. Gopalakrishnan, K. Hausman, A. Herzog, D. Ho, J. Hsu, J. Ibarz, B. Ichter, A. Irpan, E. Jang, R. Ruano, K. Jeffrey, and A. Zeng. Do as i can, not as i say: Grounding language in robotic affordances. In *Proceedings of the Conference on Robot Learning*, 2023. 2
- [2] Inhwon Bae, Junoh Lee, and Hae-Gon Jeon. Can language beat numerical regression? language-based multimodal trajectory prediction. In *Proceedings of the Computer Vision and Pattern Recognition Conference*, pages 753–766, 2024. 2, 3
- [3] Jinze Bai, Shuai Bai, Shusheng Yang, Shijie Wang, Sinan Tan, Peng Wang, Junyang Lin, Chang Zhou, and Jingren Zhou. Qwen-vl: A versatile vision-language model for understanding, localization, text reading, and beyond. *arXiv preprint arXiv:2308.12966*, 2023. 4
- [4] A. Brohan, N. Brown, J. Carbajal, Y. Chebotar, J. Dabis, C. Finn, K. Gopalakrishnan, K. Hausman, A. Herzog, J. Hsu, J. Ibarz, B. Ichter, A. Irpan, N. J. Joshi, R. Julian, D. Kalashnikov, Y. Kuang, I. Leal, L. Lee, and A. Zeng. Rt-2: Vision-language-action models transfer web knowledge to robotic control. In *Proceedings of the Conference on Robot Learning*, pages 2165–2183, 2023. 2
- [5] Konstantinos Charalampous, Ioannis Kostavelis, and Antonios Gasteratos. Robot navigation in large-scale social maps: An action recognition approach. *Expert Systems with Applications*, 66(30):261–273, 2016. 2
- [6] Yu Fan Chen, Michael Everett, Miao Liu, and Jonathan P. How. Socially aware motion planning with deep reinforcement learning. In *Proceedings of the IEEE/RSJ International Conference on Intelligent Robots and Systems*, pages 1343–1350, 2017. 1, 2
- [7] Pranav Singh Chib and Pravendra Singh. Lg-traj: Llm guided pedestrian trajectory prediction. In *ICCV 2025 Workshop on Curated Data for Efficient Learning (CDEL)*, pages 6802–6812, 2025. 2
- [8] Pei-Huai Ciou, Yu-Ting Hsiao, Zong-Ze Wu, Shih-Huan Tseng, and Li-Chen Fu. Composite reinforcement learning for social robot navigation. In *Proceedings of the IEEE/RSJ International Conference on Intelligent Robots and Systems*, pages 2553–2558, 2018. 1, 2
- [9] Tim Dettmers, Mike Lewis, Sam Shleifer, and Luke Zettlemoyer. 8-bit optimizers via block-wise quantization. In *Proceedings of the International Conference on Learning Representations*, 2022. 5
- [10] Tim Dettmers, Artidoro Pagnoni, Ari Holtzman, and Luke Zettlemoyer. Qlora: Efficient finetuning of quantized llms. *Advances in Neural Information Processing Systems*, 36:10088–10115, 2023. 5
- [11] D. Driess, F. Xia, M. S. M. Sajjadi, C. Lynch, A. Chowdhery, B. Ichter, A. Wahid, J. Tompson, Q. Vuong, T. Yu, W. Huang, Y. Chebotar, P. Sermanet, D. Duckworth, S. Levine, V. Vanhoucke, K. Hausman, M. Toussaint, K. Greff, and P. Florence. Palm-e: An embodied multimodal language model. In *Proceedings of the International Conference on Machine Learning*, 2023. 2
- [12] Gonzalo Ferrer, Anaís Garrell, and Alberto Sanfeliu. Robot companion: A social-force based approach with human awareness-navigation in crowded environments. In *Proceedings of the IEEE/RSJ International Conference on Intelligent Robots and Systems*, Tokyo, Japan, 2013. 2
- [13] Daniel Floegel, Marcos Gomez Villafane, Joshua Ransiek, and Soren Hohmann. Disentangling uncertainty for safe social navigation using deep reinforcement learning. In *Proceedings of the IEEE/RSJ International Conference on Intelligent Robots and Systems*, 2025. 1, 2
- [14] D. Gonon and A. Billard. Inverse reinforcement learning of pedestrian-robot coordination. *IEEE Robotics and Automation Letters*, 8(8):4815–4822, 2023. 1, 2
- [15] Nate Gruver, Marc Finzi, Shikai Qiu, and Andrew Gordon Wilson. Large language models are zero-shot time series forecasters. *Advances in Neural Information Processing Systems*, 36:19622–19635, 2023. 2
- [16] Dirk Helbing and Péter Molnár. Social force model for pedestrian dynamics. *Physical Review E*, 51(5):4282, 1995. 2
- [17] Noriaki Hirose, Fei Xia, Roberto Martín-Martín, Amir Sadeghian, and Silvio Savarese. Deep visual mpc-policy learning for navigation. *IEEE Robotics and Automation Letters*, 4(4):3184–3191, 2019. 1, 5, 6
- [18] Jyh-Jing Hwang, Runsheng Xu, Hubert Lin, Wei-Chih Hung, Jingwei Ji, Kristy Choi, Di Huang, Tong He, Paul Covington, Benjamin Sapp, Yin Zhou, James Guo, Dragomir Anguelov, and Mingxing Tan. EMMA: End-to-end multimodal model for autonomous driving. *Transactions on Machine Learning Research*, 2025. 2
- [19] Ming Jin, Shiyu Wang, Lintao Ma, Zhixuan Chu, James Y. Zhang, Xiaoming Shi, Pin-Yu Chen, Yuxuan Liang, Yuanfang Li, Shirui Pan, and Qingsong Wen. Time-llm: Time series forecasting by reprogramming large language models. In *Proceedings of the International Conference on Learning Representations*, 2024. 2
- [20] Haresh Karnan, Anirudh Nair, Xuesu Xiao, Garrett Warnell, Soren Pirk, Alexander Toshev, Justin Hart, Joydeep Biswas, and Peter Stone. Socially compliant navigation dataset (scand): A large-scale dataset of demonstrations for social navigation. *IEEE Robotics and Automation Letters*, 7(4):11807–11814, 2022. 1, 5, 7, 8
- [21] Tribhi Kathuria, Ke Liu, Junwoo Jang, X. Jessie Yang, and Maani Ghaffari. Learning implicit social navigation behavior using deep inverse reinforcement learning. *IEEE Robotics and Automation Letters*, 10(5):5146–5153, 2025. 1, 2
- [22] Moo Jin Kim, Karl Pertsch, Siddharth Karamcheti, Ted Xiao, Ashwin Balakrishna, Suraj Nair, Rafael Rafailov, Ethan Foster, Grace Lam, Pannag Sanketi, Quan Vuong, Thomas Kollar, Benjamin Burchfiel, Russ Tedrake, Dorsa Sadigh, Sergey

- Levine, Percy Liang, and Chelsea Finn. Openvla: An open-source vision-language-action model. *arXiv preprint arXiv:2406.09246*, 2024. 1
- [23] Teyun Kwon, Norman Di Palo, and Edward Johns. Language models as zero-shot trajectory generators. *IEEE Robotics and Automation Letters*, 9(7):6728–6735, 2024. 2, 3
- [24] Zhonghang Li, Lianghao Xia, Jiabin Tang, Yong Xu, Lei Shi, Long Xia, Dawei Yin, and Chao Huang. Urbangpt: Spatio-temporal large language models. In *Proceedings of the 30th ACM SIGKDD Conference on Knowledge Discovery and Data Mining*, pages 5351–5362, 2024. 2, 6, 7
- [25] Shubo Liu, Hongsheng Zhang, Yuankai Qi, Peng Wang, Yaning Zhang, and Qi Wu. Aerialvln: Vision-and-language navigation for uavs. In *Proceedings of the IEEE/CVF International Conference on Computer Vision*, pages 15384–15394, 2023. 1
- [26] Xu Liu, Junfeng Hu, Yuan Li, Shizhe Diao, Yuxuan Liang, and Bryan Hooi. Unitime: A language-empowered unified model for cross-domain time series forecasting. In *Proceedings of the ACM Web Conference*, pages 4095–4106, 2024. 2
- [27] Xinhao Liu, Jintong Li, Yicheng Jiang, Niranjana Sujay, Zhicheng Yin, Juexiao Zhang, John Abanes, Jing Zhang, and Chen Feng. Citywalker: Learning embodied urban navigation from web-scale videos. In *Proceedings of the Computer Vision and Pattern Recognition Conference*, pages 6875–6885, 2025. 1, 2, 5, 6
- [28] Yong Liu, Guo Qin, Xiangdong Huang, Jianmin Wang, and Mingsheng Long. Autotimes: Autoregressive time series forecasters via large language models. In *Advances in Neural Information Processing Systems*, pages 122154–122184, 2024. 2
- [29] Ilya Loshchilov and Frank Hutter. Decoupled weight decay regularization. *arXiv preprint arXiv:1711.05101*, 2017. 5
- [30] Kaiwei Luo and Jiliu Zhou. Large language models for single-step and multi-step flight trajectory prediction. *arXiv preprint arXiv:2501.17459*, 2025. 2, 3
- [31] Tian Ma, Yixuan Zhao, Minda Li, Yue Chen, Fangshu Lei, Yanan Zhao, and Maazen Alsabaan. TPLLM: A traffic prediction framework based on pretrained large language models. *Applied Soft Computing*, 184, 2025. 2, 6
- [32] Roberto Martín-Martín, Mihir Patel, Hamid Rezatofighi, Abhijeet Shenoi, JunYoung Gwak, and Eric Frankel. Jrdb: A dataset and benchmark of egocentric robot visual perception of humans in built environments. *IEEE Transactions on Pattern Analysis and Machine Intelligence*, 45(6):6748–6765, 2023. 1
- [33] Duc M. Nguyen, Mohammad Nazeri, Amirreza Payandeh, Aniket Datar, and Xuesu Xiao. Toward human-like social robot navigation: A large-scale, multi-modal, social human navigation dataset. In *Proceedings of the IEEE/RSJ International Conference on Intelligent Robots and Systems*, pages 7442–7447, 2023. 1
- [34] Fei Ni, Jianye Hao, Shiguang Wu, Longxin Kou, Jiashun Liu, Yan Zheng, Bin Wang, and Yuzheng Zhuang. Generate subgoal images before act: Unlocking the chain-of-thought reasoning in diffusion model for robot manipulation with multimodal prompts. In *Proceedings of the Computer Vision and Pattern Recognition Conference*, 2024. 2
- [35] Bhabaranjan Panigrahi, Amir Hossain Raj, Mohammad Nazari, and Xuesu Xiao. A study on learning social robot navigation with multimodal perception. In *arXiv preprint arXiv:2309.12568*, 2023. 2
- [36] Amirreza Payandeh, Daeun Song, Mohammad Nazeri, Jing Liang, Praneel Mukherjee, Amir Hossain Raj, Yangzhe Kong, Dinesh Manocha, and Xuesu Xiao. Social-llava: Enhancing robot navigation through human-language reasoning in social spaces. In *arXiv preprint arxiv.2501.09024*, 2024. 2
- [37] Alec Radford, Jong Wook Kim, Chris Hallacy, Aditya Ramesh, Gabriel Goh, Sandhini Agarwal, Girish Sastry, Amanda Askell, Pamela Mishkin, Jack Clark, Gretchen Krueger, and Ilya Sutskever. Learning transferable visual models from natural language supervision. In *Proceedings of the International Conference on Machine Learning*, 2021. 5
- [38] Sunil Srivatsav Samsani and Mannan Saeed Muhammad. Socially compliant robot navigation in crowded environment by human behavior resemblance using deep reinforcement learning. *IEEE Robotics and Automation Letters*, 6(3):5223–5230, 2021. 1, 2
- [39] Dhruv Shah, Benjamin Eysenbach, Nicholas Rhinehart, and Sergey Levine. Rapid exploration for open-world navigation with latent goal models. In *Proceedings of 5th Annual Conference on Robot Learning*, pages 674–684, 2022. 1, 5, 6, 8
- [40] Dhruv Shah, Błażej Osiański, Brian Ichter, and Sergey Levine. Lm-nav: Robotic navigation with large pre-trained models of language, vision, and action. In *Proceedings of the Conference on Robot Learning*, pages 492–504, 2023. 1
- [41] Dhruv Shah, Ajay Sridhar, Arjun Bhorkar, Noriaki Hirose, and Sergey Levine. Gnm: A general navigation model to drive any robot. In *Proceedings of the IEEE International Conference on Robotics and Automation*, page 7226–7233, 2023. 5, 6
- [42] NDhruv Shah, Ajay Sridhar, Nitish Dashora, Kyle Stachowicz, Kevin Black, Noriaki Hirose, and Sergey Levine. Vint: A foundation model for visual navigation. In *Proceedings of the Conference on Robot Learning*, pages 711–733, 2023. 1, 2, 5, 6
- [43] Ajay Sridhar, Dhruv Shah, Catherine Glossop, and Sergey Levine. Nomad: Goal masked diffusion policies for navigation and exploration. In *Proceedings of the IEEE International Conference on Robotics and Automation*, pages 63–70, 2024. 1, 2, 5, 6
- [44] Shu Wang, Muzhi Han, Ziyuan Jiao, Zeyu Zhang, Ying Nian Wu, Song-Chun Zhu, and Hangxin Liu. Llm<sup>3</sup>: Large language model-based task and motion planning with motion failure reasoning. In *2024 IEEE/RSJ International Conference on Intelligent Robots and Systems (IROS)*, pages 12086–12092, 2024. 2, 3
- [45] Jason Wei, Yi Tay, Rishi Bommasani, et al. Chain-of-thought prompting elicits reasoning in large language models. In *Advances in Neural Information Processing Systems*, pages 24824–24837, 2022. 2

- [46] Micha Zawalski, William Chen, Karl Pertsch, Oier Mees, Chelsea Finn, and Sergey Levine. Robotic control via embodied chain-of-thought reasoning. In *Proceedings of the Conference on Robot Learning*, pages 3157–3181, 2025. [2](#)
- [47] Yuanhan Zhang, Jinming Wu, Wei Li, Bo Li, Zejun Ma, Ziwei Liu, and Chunyuan Li. Video instruction tuning with synthetic data. *Transactions on Machine Learning Research*, 2025. [3](#), [5](#), [6](#), [7](#)
- [48] Xinxin Zhao, Wenzhe Cai, Likun Tang, and Teng Wang. Imaginnav: Prompting vision-language models as embodied navigator through scene imagination. In *Proceedings of the International Conference on Learning Representations*, 2025. [1](#)
- [49] Gengze Zhou, Yicong Hong, and Qi Wu. Navgpt: Explicit reasoning in vision-and-language navigation with large language models. In *Proceedings of the AAAI Conference on Artificial Intelligence*, pages 7641–7649, 2024. [1](#)
- [50] Tian Zhou, Peisong Niu, Xue Wang, Liang Sun, and Rong Jin. One fits all: Power general time series analysis by pre-trained lm. In *Advances in Neural Information Processing Systems*, 2023. [2](#)
- [51] K. Zhu, B. Li, W. Zhe, and T. Zhang. Collision avoidance among dense heterogeneous agents using deep reinforcement learning. *IEEE Robotics and Automation Letters*, 8(1): 57–64, 2023. [1](#), [2](#)